Journal of Power Sources 193 (2009) 822–827

Contents lists available at ScienceDirect

Journal of Power Sources

journal homepage: www.elsevier.com/locate/jpowsour

Physical and electrochemical properties of $LiFePO_4$/C composite cathode prepared from various polymer-containing precursors

Yao-Hong Nien, James R. Carey, Jenn-Shing Chen*

Department of Applied Chemistry, National University of Kaohsiung, Kaohsiung City 811, Taiwan, ROC

ARTICLE INFO

Article history:
Received 26 November 2008
Received in revised form 11 March 2009
Accepted 13 April 2009
Available online 22 April 2009

Keywords:
$LiFePO_4$
Polymer additive
Cathode material
Coprecipitation

ABSTRACT

The goal of this research was to study the effect of various polymer-containing precursors on the performance of $LiFePO_4$/C composite. A coprecipitation method was applied to prepare a series of $LiFePO_4$/C materials by calcinating amorphous $LiFePO_4$ with various polymer compounds at 600 °C. The materials were characterized by X-ray diffraction, scanning electron microscopy, transmission electron microscopy, particle size analysis, thermal analysis, BET specific surface area, Raman spectral analysis and electrochemical methods. The results showed that the structure of polymer precursors played an important role in improving the performance of $LiFePO_4$/C composites. The residual carbon produced by the pyrolysis of polymers with functionalized aromatic groups exhibited a better capacity in the $LiFePO_4$/C composites. A polyaromatic compound, e.g. polystyrene, with more functionalized aromatic groups displayed improved performance because its decomposition temperature was close to the temperature of the $LiFePO_4$ phase transformation, which resulted in fine particle size and uniform carbon distribution on the composite surface. According to Raman spectral analysis, polystyrene with more aromatic groups has a lower I_D/I_G and sp^3/sp^2 peak ratio indicating more highly graphite-like carbon formation during polymer pyrolysis and exhibited a better capacity.

© 2009 Elsevier B.V. All rights reserved.

1. Introduction

In recent years, olivine $LiFePO_4$ has been extensively studied as a cathode material for Li-ion batteries because of its high theoretical capacity (170 mAh g^{-1}), cycling stability, low cost, and environmental friendliness. Unfortunately, the poor rate performance of $LiFePO_4$ limits its practical application. The major reason for its poor rate capability can be attributed to its intrinsically poor electronic conductivity (on the order of 10^{-9} S cm^{-2}) [1–3]. To overcome these problems, several strategies have been implemented such as optimization of synthetic procedures [4], carbon nanocoating [5,6], particle size minimization [7], metal powder addition [8,9] and doping with supervalent ions [10] or carbothermal formation of the surface conducting phase [10–12]. To date, most of the improvements to the rate capacity of $LiFePO_4$ have focused on the incorporation of conductive carbon into active material powders to form carbon-coated $LiFePO_4$ ($LiFePO_4$/C) composites.

The behavior of $LiFePO_4$/C composites depend on the phase purity of the active material, particle size, structure of the carbon additive, the amount of carbon content, the form of carbon contact, and the mixing and sintering recipe. The performance of LiFePO4/C composites related to the carbon structural parameters derived from Raman analysis of samples has recently been investigated [12–15]. The data suggests that the selected carbon precursors directly affected the characteristics of the carbon additive, which is proportional to the performance of the LiFePO4/C composite. Polymer pyrolysis is a well-known method and was successfully applied to many ceramic systems to form carbon-coated particles (ceramic/carbon composites), e.g. Al_2O_3, SiO_2, MgO, TiO_2, Fe_3O_4, Fe_2O_3, NiO_2, Co_3O_4, ZnO, and CaO [16–21]. During the pyrolysis of polymers in an inert atmosphere, some residual carbon remained in the system. It was reported that the selection of the carbon source, or polymer precursor, is very important for tailoring the final properties of carbon-coated composite powders.

Described here, are carbon-coated $LiFePO_4$ powders that were prepared via polymer pyrolysis. Various polymer-containing precursors were studied to understand their influence on the behavior of $LiFePO_4$/C composites. Recently, it was found that more highly graphitized carbons are formed during pyrolysis when functionalized aromatic or ring-forming compounds were used [12–15]. Thus, two major types of polymer compounds were studied including vinyl polymers with ring or aromatic functional groups, such as polyethylene oxide (PEO), polystyrene (PS) and vinylphenyl /or unsaturated polymer or block copolymer, such as polybutadiene (PB) and styrene–butadiene–styrene (SBS). The vinyl polymers are known to be carbonized through a liquid phase with very low viscosity, which allows for coating with uniform carbonaceous layers [16,22]. During the pyrolysis of vinylphenyl or unsaturated poly-

* Corresponding author. Tel.: +886 7 591 9463; fax: +886 7 591 9348.
E-mail address: jschen@nuk.edu.tw (J.-S. Chen).

0378-7753/$ – see front matter © 2009 Elsevier B.V. All rights reserved.
doi:10.1016/j.jpowsour.2009.04.013

mers, scissions of the main chain without the evolution of volatile products take place and the charring process of unsaturated bond and aromatic rings favor of the formation of graphite [22–24]. In addition, the thermal behavior of SBS block copolymer resembles the corresponding PS and PB homoploymers. Therefore, four polymers, PEO, PS, PB and SBS were investigated to assess their additive effects in this study.

A coprecipitation method was adopted to prepare $LiFePO_4$ and its carbon composites because of its simplicity and low cost [15]. Moreover, it was easy to control the amount and characteristics of residual carbon on the surface of $LiFePO_4$ particle from the source of various polymer compounds. In order to obtain uniform carbon distribution, *in situ* coating of carbon from the pyrolysis of polymer additives on the $LiFePO_4$ particle surfaces was performed. During the synthesis of composites, the polymer additives were dissolved in a solvent first, and then homogeneously mixed with the amorphous $LiFePO_4$ particles before the final heating step. From the pyrolysis of various polymer compounds, a series of residual carbons on the surface of prepared $LiFePO_4$ materials were characterized. In addition, the electrochemical properties of as-prepared $LiFePO_4$/C composites as cathodes in lithium-ion cells were measured from cyclic voltammogram (CV) and charge–discharge tests.

2. Experimental

$LiFePO_4$ and its carbon composites were prepared by a co-precipitation method in de-ionized water at room temperature. The modified method of Prosini and co-workers [15,25] was applied to synthesize $LiFePO_4$/C composites. Amorphous $LiFePO_4$ was obtained by the chemical lithiation of amorphous $FePO_4$ using Li as a reducing agent. A detailed preparation procedure can be found in ref. [15]. The solutions of carbon additive precursors prepared by dissolving different polymer compounds in a selected solvent are listed in Table 1. Proper amounts of polymer solutions were mixed homogeneously with amorphous $LiFePO_4$ particles and were heat-treated in a tubular furnace at 600 °C for 8 h under reducing atmosphere ($Ar/H_2 = 95/5$) to yield $LiFePO_4$/C composite materials.

A Rigaku-D/MaX-2550 diffractometer with Cu K_α radiation ($\lambda = 1.54$ Å) was used to obtain X-ray diffraction (XRD) patterns for the samples. The morphology of the sample was observed by a scanning electron microscope (SEM, Hitachi S-4300) and transmission electron microscope (TEM, JEOL JEM-2010). Particle size analysis (PSA) was carried out with a Malvern particle size analyzer (Zetasizer Nano ZS). An integrated Raman microscope system "JOBIN-YVON T64000" was used to analyze the structure and composition of the individual particles in $LiFePO_4$. Thermogravimetry (TG) apparatus (SETARAM) was used for the thermal analysis. The specific surface area was measured by using a Brunauer–Emmett–Teller (BET) apparatus (ASAP2020). The residual carbon content of the powders was determined by means of an automatic elemental analyzer (Elementar vario, EL III).

For electrochemical evaluation, the composite electrodes were prepared by wet coating, and were made from as-prepared $LiFePO_4$/C with acetylene black, SFG-6 synthetic flake graphite (Timcal Ltd.), and polyvinylidene fluoride (PVDF) binder (MKB-212C, Elf Atochem) in a weight ratio of 80:5:5:10. The $LiFePO_4$/C active materials, acetylene black and SFG-6 were first added to a solution of PVDF in *n*-methyl-2-pyrrolidone (NMP, Riedel-deHaen). The mixture is stirred for 20 min at room temperature with a magnetic bar, and then with a turbine for 5 min at 2000 rpm to make a slurry with an appropriate viscosity. The resulting slurry was coated onto a piece of aluminum foil and dried at 120 °C for 40 min. The coating had a thickness of ~100 μm with an active material mass loading of 8 ± 1 mg cm^{-2}. The quantity of active materials on the electrodes was kept constant. Electrodes were dried overnight at 100 °C under vacuum before being transferred to an argon-filled glove box for cell assembly. Electrodes were placed in an open glass bottle cell with a 1 cm^2 square $LiFePO_4$/C cathode electrode and lithium foil as the counter and reference electrodes for CV experiment. Coin cells of 2032 size were assembled using lithium metal as a counter electrode. A solution of 1 M $LiPF_6$ in a mixed solvent of ethylene carbonate/dimethyl carbonate (EC/DMC) with 1:1 volume ratio was used as the electrolyte in all cells. The CV experiment was carried out with a CHI 704A potentiostat at a scan rate of 0.1 mV s^{-1}. Coin cells were cycled galvanostatistically with a BAT-750B (Acu Tech System) at a constant current of 0.5*C* with a voltage region of 2.5–4.2 V vs. Li/Li$^+$ at room temperature; here, 1*C* equals 170 mA g^{-1}. The current density was calculated based on the mass of $LiFePO_4$/C in the electrode.

3. Results and discussion

The carbon-coated $LiFePO_4$ ($LiFePO_4$/C) electrode was chosen for this study because of its enhanced conductivity over normal $LiFePO_4$. Many authors [15–23] have reported that the polymer pyrolysis method is a relatively simple method for coating fine particles via a carbon layer, and the type of polymer precursors is an important parameter which directly affects the final quality of carbon-coated composite powders. The polymer pyrolysis method was used to prepare $LiFePO_4$/C composites. Various types of polymer precursors as carbon sources were investigated to understand the influence of electrochemical performance and physical properties of the composite materials. Four types of polymer additives,

Table 1
$LiFePO_4$ samples processed with polymer additives.

Polymer additive	Chemical formula	Solvent	Supplier/molecular weight (M_w)
PEO	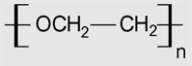	DI water	Aldrich /300,000
PB	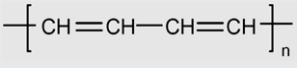	Toluene	TAIPOL™/200,000
PS	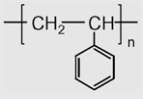	Toluene	Aldrich/280,000
SBS (SM:BD = 34:66)	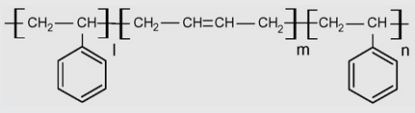	Toluene	TAIPOL™/250,000

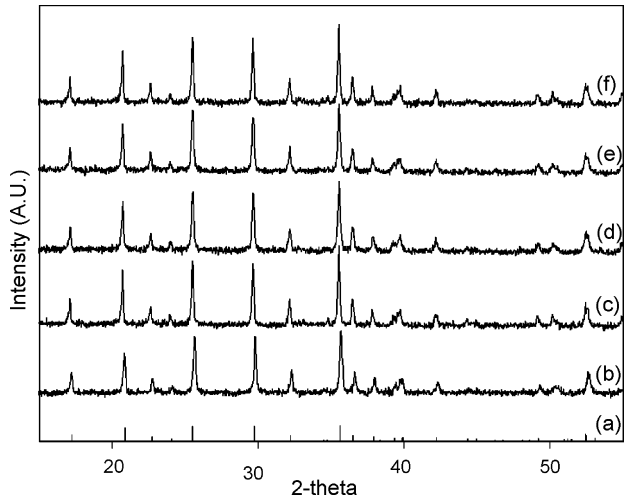

Fig. 1. XRD patterns of $LiFePO_4$/C composites prepared from different polymer pyrolysis (a) theoretical pattern, (b) pure $LiFePO_4$, (c)PEO, (d)PB, (e)PS, (f)SBS.

PEO, PS, PB, and SBS, were studied to assess their additive effects. The structures of polymer compounds and their solvents are listed in Table 1. In order to avoid different amounts of residual carbon in the composites, a series of samples was synthesized by calcinating amorphous $LiFePO_4$ with proper amounts of polymer at 600 °C. The final amount of residual carbon was controlled to be about 2 wt% for all samples.

All of $LiFePO_4$/C composite materials are deep black in color, in contrast to the gray color of $LiFePO_4$ powders. Fig. 1 shows the XRD patterns of the prepared samples. All peaks can be indexed as a single phase with an ordered olivine structure indexed to the orthorhombic *Pnmb* space group. The XRD curves did not show any evidence of the formation of crystalline or amorphous carbon. It appears that using polymers as a carbon source most likely remains amorphous or as low crystalline carbon in the final product.

Various polymer compounds were thermally analyzed in order to examine the effect of their thermal decomposition on the behavior of the composites. The TG curves of all powder mixtures consisting of amorphous $LiFePO_4$ with various polymer-containing precursors recorded at a scanning rate of 5 °C min^{-1} under N_2 flow are shown in Fig. 2. In the TG curves, all polymer compounds exhibit appreciable, rapid, weight-loss over a range of temperature that corresponds to the pyrolysis and decomposition. However,

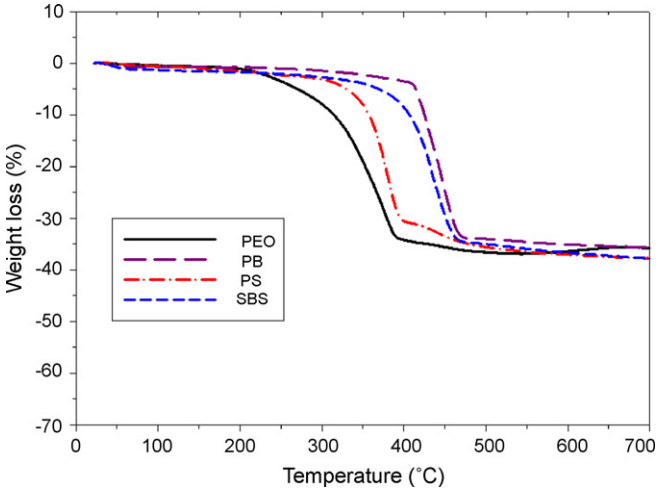

Fig. 2. TGA of various polymer-containing precursors measured at a heating rate of 5 °C min^{-1} in nitrogen at a 60 mL min^{-1} flow rate.

Table 2
Comparison of decomposition temperature at 600 °C, residual carbon content and surface area for $LiFePO_4$/C powders via various polymer pyrolysis.

Polymer additives (wt%)	Decomposed temperature (°C)	Residual carbon content (wt%)	BET surface area (m^2 g^{-1})
25% PEO	240–380	2.2	10.4
3% PB	410–470	2.2	27.4
5% PS	320–480	1.8	19.8
3% SBS	350–465	2.0	16.0

after the range of decomposition temperatures, a small gradual weight-loss is observed because the pyrolysis of the remaining polymers continues until 600 °C. This also indicates that the polymer compounds were decomposed rather than evaporated during successive thermal treatments. The final quantity of residual carbon (about 2 wt%) for pyrolysis of all polymers were measured by an elemental analyzer (EA). Table 2 presents the decomposition temperature range, residual carbon content and BET surface area for various polymer compounds. Taken together, these data strongly suggest that the differences in the structures of polymer compounds affect the decomposition temperature range. The transformation temperature from an amorphous to a crystalline phase of a $LiFePO_4$ compound has been studied at ~470 °C [26–28]. There is an obvious correlation between the electrochemical capacity of $LiFePO_4$/C composites and temperature difference between the decomposition of organic compounds and the phase transformation of $LiFePO_4$ [15,26]. As mentioned in our previous study [15], while the temperature difference is small, a synchronous process of $LiFePO_4$ crystallization and polymer pyrolysis occurs like an *in situ* synthesis of the $LiFePO_4$/C composite, and the highly active carbon from the pyrolysis of polymer compounds homogeneously coated on the surface of a fresh crystallized $LiFePO_4$ particle hinders the particle growth efficiently causing the formation of a composite with a fine particle size and uniform carbon distribution on the surface. The TG curves show that the decomposition temperatures of PB and PS are close to the temperature of the $LiFePO_4$ phase transformation. Both polymer compounds outperformed all other polymer compounds in this study because their decomposition temperatures are close to the temperature of $LiFePO_4$ phase transformation.

Fig. 3 shows the SEM images of the $LiFePO_4$/C composites with (a) PEO, (b) PB, (c) PS, and (d) SBS. The general appearances of $LiFePO_4$/C composites are mostly homogeneous with carbon surrounding the $LiFePO_4$ particles, although a few agglomerates exist. The composites appear to be framed by an amorphous carbon matrix with the $LiFePO_4$ particles captured inside. The mean particle size of all samples, as determined by PSA, is in the range of 200–400 nm which is in good agreement with the SEM measurement. The data from the BET measurement shown in Table 2, gives a specific surface area of about 10.4, 27.4, 19.8 and 16.0 m^2 g^{-1} for the crystalline material from PEO, PB, PS and SBS, respectively. PEO has a larger particle sizes, which results in smaller surface area of the composite. In our previous work [15], an increase in residual carbon content or synchronous process of $LiFePO_4$ crystallization and carbon precursor pyrolysis will suppress the growth of $LiFePO_4$/C particles and increases homogeneity. In this work, all polymer samples were controlled with similar residual carbon content at ~2 wt%. Thus, like the results of TG analysis (Fig. 2), PB and PS pyrolysis occur like an *in situ* synthesis of the $LiFePO_4$/C composite causing the formation of a composite with a fine particle size and uniform carbon distribution on the surface.

The TEM micrograph of $LiFePO_4$/C composite obtained by the pyrolysis of SBS is shown in Fig. 4. The relatively dark portion shown in the figure represents $LiFePO_4$ with particle size between 100 and 200 nm, and these particles were surrounded by carbon matrix that was light gray in color. From the TEM images, it can be clearly seen

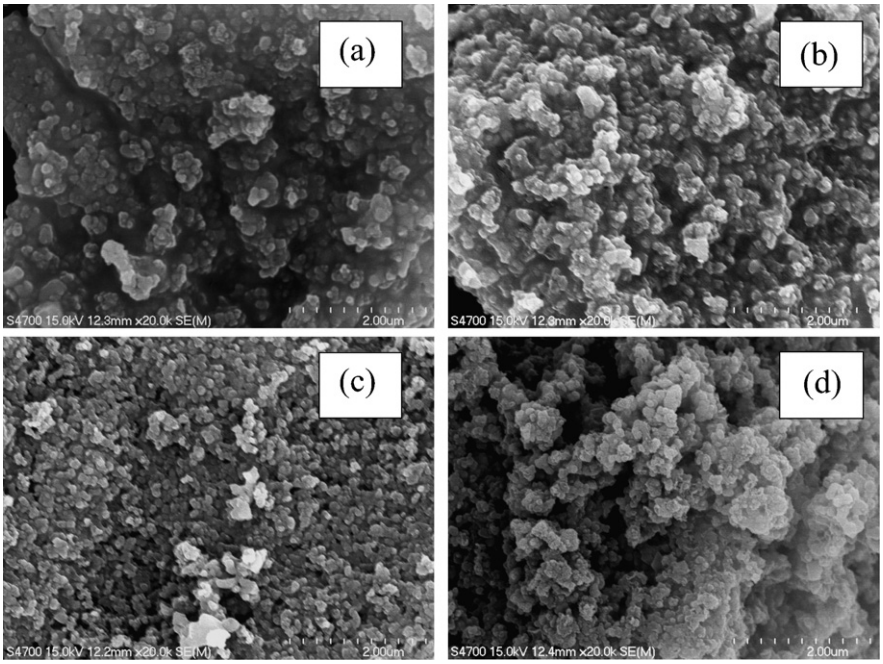

Fig. 3. SEM images of $LiFePO_4$/C composites containing samples (a) PEO, (b) PB, (c) PS, and (d) SBS.

that the entire carbon distribution surrounds the fine $LiFePO_4$ crystal grains like a web made of carbon. This "carbon web" leads to electronic inter-grain connection, but does not block the direct contact between the active particles and the encapsulated electrolyte. Moreover, all samples exhibited small but various coating thickness on the $LiFePO_4$ particles, which were in the range of 20–70 nm. As shown in Fig. 4, the thickness of the carbon coating on SBS was estimated about 30–50 nm. Recent studies [12,13,15] have shown the thickness of coating carbon and structure of residual carbon play important roles in controlling the performance of the $LiFePO_4$/C composite. According to this work, the main factor controlling the performance of the $LiFePO_4$/C composite is the structure of what is deposited on the particle.

The CV plots of various $LiFePO_4$/C electrodes in the beaker cell cycled between 3.0 and 4.0 V with 0.1 mV s^{-1} and 1 M $LiBF_4$ + EC/DMC (1:1) electrolyte are shown in Fig. 5. The CV curves of all samples exhibited two peaks located at 3.6–3.8 V in the anodic sweep and 3.1–3.3 V in the cathodic sweep, consistent with a two-phase redox reaction at about 3.5 V vs. Li/Li^+. No other peaks are observed, indicating the absence of electroactive iron impurities. According to the estimation of CV curves (2nd cycle), all samples have a similar coulombic efficiency of 97–99%. However, the peak intensities or discharge capacities are variable. The composite with PS indicated a higher capacity than those with other polymers. The difference in cell capacity can be attributed to the effect of the structure of the polymer compounds on the surface carbon on the $LiFePO_4$/C composite. Recently, it has been reported that carbon additives produced by the pyrolysis of functionalized aromatic compounds exhibited a better capacity in the $LiFePO_4$/C composite [12,13,15]. PS, a polyaromatic compound, exhibited the best electrochemical performance.

Fig. 6 shows the charge–discharge voltage profiles of $Li/LiFePO_4$ cells containing different polymer additives at 0.1 C rate between 2.5 and 4.2 V at the 2nd cycle. A charge–discharge curve plateau over a wide voltage range at approximately 3.4 V (vs. Li/Li^+) implies that a two-phase Fe^{3+}/Fe^{2+} redox reaction proceeds via a first-order transition between $FePO_4$ and $LiFePO_4$. The small voltage difference between the charge–discharge plateaus indicates its good kinetics. As shown in Fig. 6, the PS sample delivers the largest charge capacity of 147 mAh g^{-1} in the second cycle and a subsequent discharge capacity of 143 mAh g^{-1}, about 84% of theoretical capac-

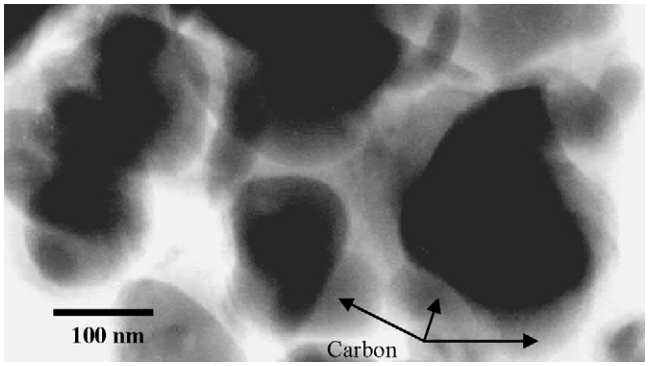

Fig. 4. TEM image of $LiFePO_4$/C composites containing SBS.

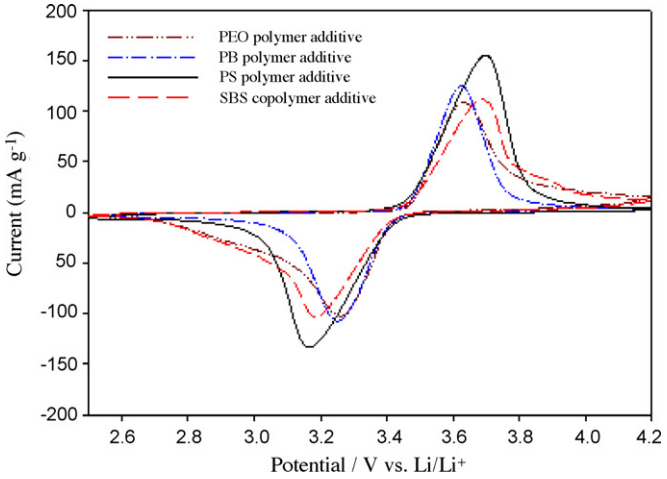

Fig. 5. CVs of Li/1 M $LiBF_4$, EC-DMC/$LiFePO_4$ cells containing different polymer additives, which were recorded in the second cycle at a scanning rate of 0.1 mV s^{-1}.

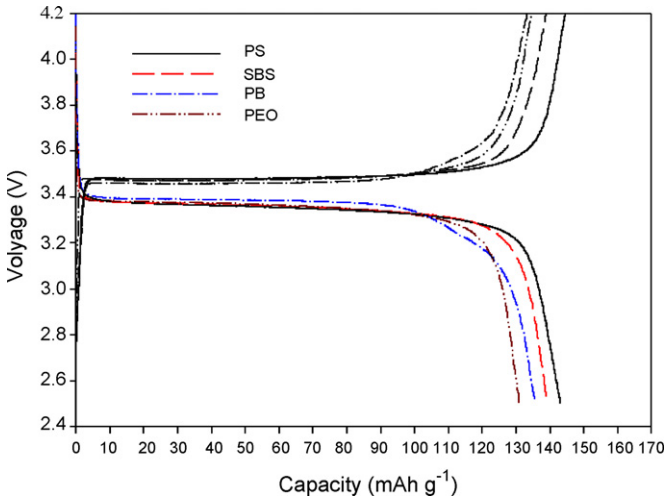

Fig. 6. Voltage profiles on the second cycle of Li/$LiFePO_4$ cells containing different polymer additives, which were recorded in the second cycle at 0.5*C* rate between 2.5 and 4.2 V.

ity (170 mAh g^{-1}). However, the PEO sample delivers the smallest charge capacity of 134 mAh g^{-1} in the 2nd cycle and a subsequent discharge capacity of 131 mAh g^{-1}. In this work, less than theoretical value of discharge capacities is associated with the larger particle size and Fe^{3+} impurities acquired during synthesis of the $LiFePO_4$/C composites [29–31]. Despite the lower discharge capacities, in the aforementioned work, we focused on the characteristics of the residual carbon from pyrolysis of various polymer compounds on the surface of the $LiFePO_4$ particles. Fig. 7 shows a plot of capacity vs. cycle number for Li/$LiFePO_4$ cells containing different polymer additives at 0.5*C* rate. The coulombic efficiency of all samples at least 97% which is in good agreement with the CV measurement. All the cells display good capacity retention after 30 cycles. However, the cell discharge capacity depends on the type of the polymer additives. Fig. 8 shows plots the discharge capacity as a function of C rate for each type of cell. All samples displayed a decreased in discharge capacity as the discharge rate was increased, indicating that there are still significant rate limitations. However, the rate of decrease, judging from the slope of the lines in Fig. 8, is less for PS than for other polymers. The difference in discharge capacity and rate capability of $LiFePO_4$/C is caused by the effect of the structure of polymer additives on the characteristic of the surface carbon on the $LiFePO_4$/C composite. Similar results were

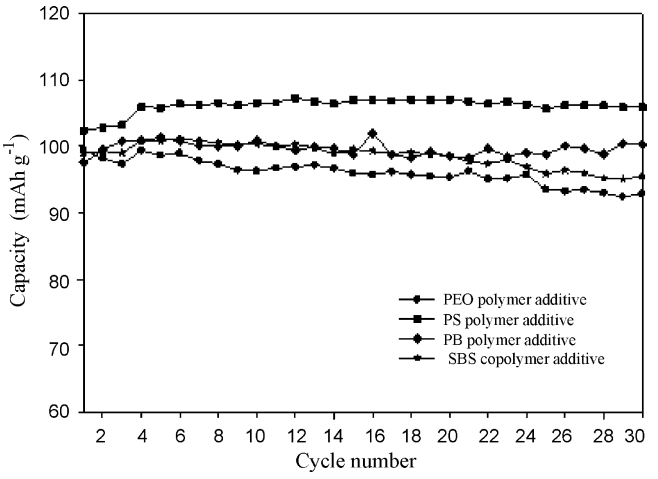

Fig. 7. Discharge capacities vs. cycle number at 0.5*C* rate between 2.5 and 4.2 V for Li/$LiFePO_4$ cells containing different polymer additives.

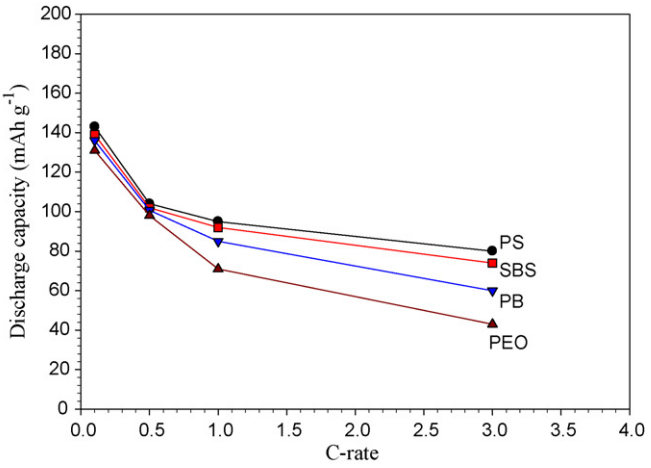

Fig. 8. Discharge capacities vs. C rate for Li/$LiFePO_4$ cells containing different polymer additives.

obtained with CV study, PS with polyaromatic structure yields the highest capacity.

The structure of the deposited carbon was investigated by Raman spectroscopy. Fig. 9 shows the Raman spectra of the $LiFePO_4$ and $LiFePO_4$/C composites with PEO, PS, PB, and SBS respectively. All spectra consisted of a relatively small band at 940 cm^{-1} corresponding to the symmetric PO_4 stretching model of $LiFePO_4$. Two intense broad bands at 1350 and 1585 cm^{-1} can be assigned to the D and G bands of residual carbon in the $LiFePO_4$/C composite, respectively. The spectrum of pure $LiFePO_4$ does not display any D and G bands, which represent the absence of any carbon content on the surface. The D and G bands were composed of four signals located at 1194, 1347, 1510, and 1585 cm^{-1} [12,13,15]. The observed spectra were analyzed by a pseudo-Voigt profile function, and separated numerically into four signals. The bands at 1347 and 1585 cm^{-1} have been assigned as the sp^2 graphite-like structure, whereas all other observed bands are attributed to the sp^3 type tetrahedral carbon, which is often observed in highly amorphous carbonaceous materials [13]. The ratio, sp^3/sp^2 was estimated to be ~0.36–0.48 for all species indicating that the fraction of graphite-like carbon was ~70% and the conducting path was mainly due to graphite-like car-

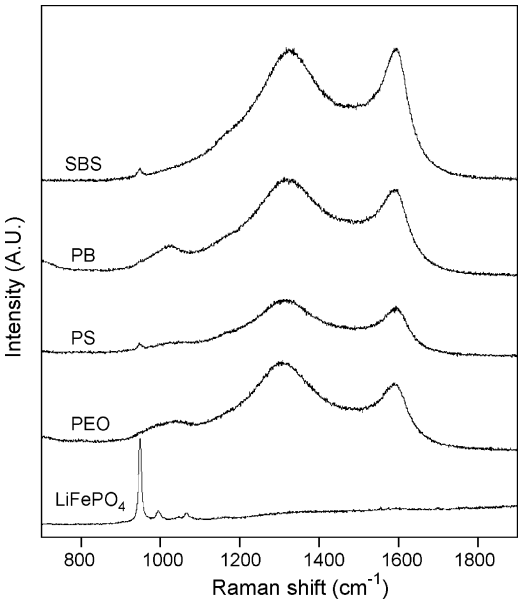

Fig. 9. Raman spectra of $LiFePO_4$ and $LiFePO_4$/C powders.

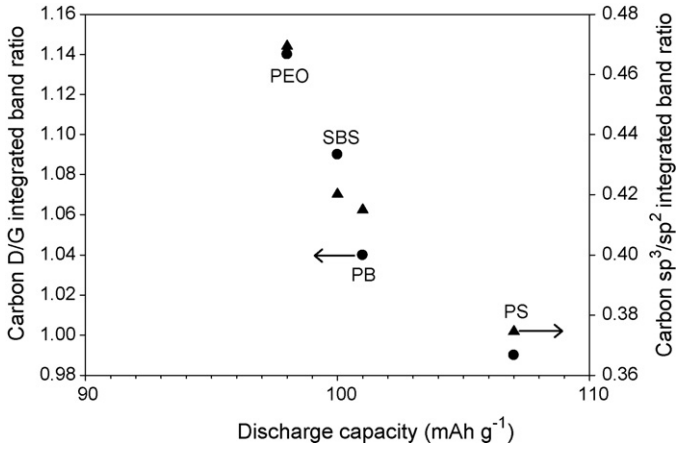

Fig. 10. Relationship of Raman intensity ratios of D/G bands and sp^3/sp^2 coordinated carbon with discharge capacity for various polymer additives ((●) D/G, (▲) sp^3/sp^2).

bon. In addition, the intensity ratio $R = I_D/I_G$ defines the level of order and the in-plan crystal size for the pyrolytic carbon. Both I_D/I_G and sp^3/sp^2 parameters as a function of different polymer compounds are shown in Fig. 10. PS with the lowest I_D/I_G and sp^3/sp^2 values exhibit the highest discharge capacities and better rate capability. In general, higher capacities and better capability are directly correlated with low values of the I_D/I_G and sp^3/sp^2 parameters. The low values for the I_D/I_G and sp^3/sp^2 parameters indicate a high degree of graphitization. The increasing degree of graphitization can improve the electronic conductivity of residual carbon and thus provide better electronic contact between submicrometer particles with large agglomerates resulting in better electrode performance. PS contains a large number of functionalized aromatic structures causing the formation of more highly graphite-like carbons during pyrolysis yielding composites with better electrochemical performance.

According to our previous investigations [15], the choice of an appropriate carbon precursor is an important factor controlling the performance of the $LiFePO_4$/C composite and the beneficial effects include (i) more carbon retention, (ii) production of carbon during a critical stage of the calcinations process to limit grain growth and increase in homogeneity, and (iii) improvement of the residual carbon structure. In this work, we find that PS is suitable for producing a $LiFePO_4$/C composite with a fine particle size, and a uniformly coated carbon conductive layer, which exhibited better electrochemical performance. The major beneficial effects for PS as a polymer additive are a synchronous process of $LiFePO_4$ crystallization and PS pyrolysis and more production of larger grapheme clusters in the disordered carbon structure. Polymers with increased functionalization of aromatics, such as PS, are suitable for producing a $LiFePO_4$/C composite with a fine particle size and a uniformly coated carbon conductive layer. These characteristics yield composites with improved electrochemical performance.

4. Conclusion

Carbon-coated $LiFePO_4$ powders containing various polymer precursors (PEO, PB, PS and SBS) were prepared via polymer pyrolysis method to study the influence of structures of polymer precursors on the behavior of materials. It showed that the effect of the structure of polymer precursors on the characteristics of the residual carbon plays an important role in improving the performance of $LiFePO_4$/C composites. The residual carbon produced by the pyrolysis of polymers with functionalized aromatic groups exhibited a better capacity in the $LiFePO_4$/C composite. PS is polyaromatic compound with more functionalized aromatic groups causing the formation of more highly graphite-like carbons during polymer pyrolysis and exhibited a higher discharge capacities and better rate capability. In order to gain a fuller understanding of the principles that affect the cell capacities and rate capability of these composites, future investigations will involve the synthesis and testing of new composites. These new composites will be synthesized using an increased number and variety of organic polymeric functionality.

Acknowledgment

The authors thank the National Science Council of Taiwan for the financial support for this work under contract no. NSC-95-2113-M-390-005-MY3.

References

[1] A.K. Padhi, K.S. Nanjundaswamy, J.B. Goodenough, J. Electrochem. Soc. 144 (1997) 1188–1194.
[2] S.-Y. Chung, J.T. Bloking, Y.-M. Chiang, Nat. Mater. 2 (2002) 123.
[3] K. Striebel, J. Shim, V. Srinivasan, J. Newman, J. Electrochem. Soc. 152 (2005) A664.
[4] G. Arnold, J. Garche, R. Hemmer, S. Strobele, C. Vogler, M. Wohlfahrt-Mehrens, J. Power Sources 247 (2003) 119–121.
[5] H. Huang, S.-C. Yin, L.F. Nazar, Electrochem. Solid State Lett. 4 (2001) A170.
[6] Z. Chen, J.R. Dahn, J. Electrochem. Soc. 149 (2002) A1184.
[7] A. Yamada, S.-C. Chung, K. Hinokuma, J. Electrochem. Soc. 148 (2001) A224.
[8] F. Croce, A.D. Epifanio, J. Hassoun, A. Deptula, T. Olczac, B. Scrosati, Electrochem. Solid Sate Lett. 5 (2002) 47.
[9] K.S. Park, J.T. Son, H.T. Chung, S.J. Kim, C.H. Lee, K.T. Kang, H.G. Kim, Solid State Commun. 129 (2004) 31.
[10] S.Y. Chung, J.T. Bloking, Y.M. Chiang, Nat. Mater. 2 (2002) 123.
[11] P.S. Herie, B. Ellis, N. Coombs, L.F. Nazar, Nat. Mater. 3 (2004) 147.
[12] M. Doeff, Y. Hu, F. McLarnon, R. Kostecki, Electrochem. Solid State Lett. 6 (2003) A207.
[13] Y. Hu, M. Doeff, R. Kostecki, R. Finones, J. Electrochem. Soc. 151 (2004) A1279–1285.
[14] T. Nakamura, Y. Miwa, M. Tabuchi, Y. Yamada, J. Electrochem. Soc. 153 (2006) A1108.
[15] Chi-Wi Ong, Yuan-Kai Lin, Jenn-Shing Chen, J. Electrochem. Soc. 154 (6) (2007) A527–A533.
[16] B. Ozkal, W. Jiang, O. Yamamoto, K. Fuda, Z.-E. Nakagawa, J. Mater. Sci. 42 (2007) 983–988.
[17] M. Inagaki, H. Miura, H. Konno, J. Eur. Ceram Soc. 18 (1998) 1011.
[18] O.P. Krivoruchko, N.I. Maksimova, V.I. Zaikovskii, A.N. Salanov, Carbon 38 (2000) 1075.
[19] M. Inagaki, K. Fujita, Y. Takeuchi, K. Oshitai, H. Iwata, H. Konno, Carbon 39 (2001) 921.
[20] F. Chen, L. Liu, Z. Shen, G.O. Xu, T.S.A. Hor, Appl. Phys. A Mater. Sci. Proc. 74 (2002) 317.
[21] B. Ozkal, O. Yamamoto, K. Fuda, Z. Nakagawa, J. Ceram. Soc. Jpn. 113 (1) (2005) 116.
[22] B. Martel, J. Appl. Polym. Sci. 35 (1988) 1213.
[23] J. Hacaloglu, T. Ersen, S. Suzer, Eur. Polym. J. 33 (1997) 199.
[24] J. Hacaloglu, T. Ersen, Rapid Commun. Mass Spectrom. 12 (1998) 1793.
[25] P.P. Prosini, M. Caeewska, S. Suaccia, P. Wisniewski, S. Passerine, M. Pasquali, J. Electrochem. Soc. 149 (2002) A886.
[26] C.H. Mi, X.B. Zhao, G.S. Cao, J.P. Tu, J. Electrochem. Soc. 152 (3) (2005) A483–A487.
[27] N. Yun, H.W. Ha, K.H. Jeong, H.Y. Park, K. Kim, J. Power Sources 160 (2006) 1361–1368.
[28] H. Liu, Y. Feng, Z. Wang, K. Wang, J. Xie, Powder Technol. 184 (2008) 313–317.
[29] K.S. Park, K.T. Kang, S.B. Lee, G.Y. Kim, Y.J. Park, H.G. Kim, Mater. Res. Bull. 39 (2004) 1803–1810.
[30] S.W. Song, R.P. Reade, R. Kostecki, K.A. Striebel, J. Electrochem. Soc. 153 (1) (2006) A12–A19.
[31] L.N. Wang, Z.G. Zhang, K.L. Zhang, J. Power Sources 167 (2007) 200–205.